

# Influence of measured and simulated basis sets on metabolite concentration estimates

Cristina Cudalbu,<sup>1</sup> Sophie Cavassila,<sup>1\*</sup> Herald Rabeson,<sup>1</sup> Dirk van Ormondt<sup>2</sup> and Danielle Graveron-Demilly<sup>1</sup>

<sup>1</sup>CREATIS-LRMN, CNRS, UMR 5220, Villeurbanne F-69621, France; Inserm, U630, Villeurbanne F-69621, France; Université de Lyon, Lyon, F-69003, France; Université Lyon 1, Villeurbanne F-69622, France; INSA-Lyon, Villeurbanne F-69621, France

<sup>2</sup>Applied Physics Department, Delft University of Technology, Delft, The Netherlands

Received 7 December 2006; Revised 27 September 2007; Accepted 22 October 2007

**ABSTRACT:** By quantification of brain metabolites, localized brain proton MRS can non-invasively provide biochemical information from distinct regions of the brain. Quantification of short-*TE* signals is usually based on a metabolite basis set. The basis set can be obtained by two approaches: (1) by measuring the signals of metabolites in aqueous solution; (2) by quantum-mechanically simulating the theoretical metabolite signals. The purpose of this study was to compare the effect of these two approaches on metabolite concentration estimates. Metabolite concentrations were quantified with the QUEST method, using both approaches. A comparison was performed with the aid of Monte Carlo studies, by using signals simulated from both basis sets. The best results were obtained when the basis set used for the fit was the same as that used to simulate the Monte Carlo signals. This comparison was also performed using *in vivo* short-*TE* signals acquired at 7 T from the central region of rat brains. The concentration estimates, with confidence intervals, obtained using both basis sets were in good agreement with values from the literature. The *in vivo* study showed that, in general, the differences between the estimates obtained with the two basis sets were not statistically significant or scientifically important. Consequently, a simulated basis set can be used in place of a measured basis set. Copyright © 2007 John Wiley & Sons, Ltd.

**KEYWORDS:** MRS; rat brain; quantification; metabolite basis set

## INTRODUCTION

Localized <sup>1</sup>H MRS can provide, by quantification of brain metabolites, biochemical information from distinct regions of the brain, which can be used to detect diseases and to monitor disease progression and treatment (1–10). By using short-*TE* localization pulse sequences, it is possible to observe metabolites with short spin–spin relaxation decay time constants (*T*<sub>2</sub>) and with coupled spin systems. Accordingly, the accurate quantification of brain metabolites is of prime importance for human and animal model studies. Well-known time and frequency-domain methods (11–16), invoking prior knowledge based on metabolite basis sets, are currently used for accurate quantification. Two alternative approaches can be used to create these basis sets: (1) theoretical meta-

bolite signals or spectra quantum-mechanically simulated for the corresponding measurement protocol and acquisition parameters (11,12,14,17,18); (2) measured signals or spectra of selected aqueous metabolite solutions used as numerical time or frequency-domain model functions (12,14,18–22).

The purpose of this study was to compare the effect of these two basis set approaches on metabolite concentration estimates. First, a direct comparison of the two metabolite basis set signals was performed. Then, the influence was evaluated using Monte Carlo and *in vivo* studies and *in vivo* quantification. To our knowledge, no such comparative study has been performed.

## METHODS

### Basis sets

The numerical time-domain model functions of the following 11 metabolites were used as prior knowledge in the processing algorithm: aspartate (Asp), creatine (Cr), choline (Cho),  $\gamma$ -aminobutyric acid (GABA), glucose (Glc), glutamate (Glu), glutamine (Gln), *N*-acetyl-aspartate (NAA), taurine (Tau), lactate (Lac) and *myo*-inositol (Ins). The model functions were obtained using two approaches:

\*Correspondence to: S. Cavassila, CREATIS-LRMN, CNRS, UMR 5220, Inserm, U630, Université de Lyon, Université Lyon 1, INSA-Lyon, Domaine Scientifique de la DOUA, 43 Boulevard du 11 Novembre 1918, 69622 Villeurbanne Cedex, France.  
E-mail: sophie.cavassila@univ-lyon1.fr

**Abbreviations used:** Asp, aspartate; Cho, choline; Cr, creatine; CRLB, Cramér–Rao lower bounds; GABA,  $\gamma$ -aminobutyric acid; Glc, glucose; Gln, glutamine; Glu, glutamate; HLSVD, Hankel-Lanczos singular value decomposition algorithm; Ins, *myo*-inositol; Lac, lactate; NAA, *N*-acetyl-aspartate; PRESS, point resolved spectroscopy; RARE, rapid acquisition with relaxation enhancement; SNR, signal-to-noise ratio; Tau, taurine; VOI, volume of interest.

(1) assembling a measured basis set comprising the measured signals of the above metabolites in aqueous solutions; (2) assembling a simulated basis set comprising the theoretical metabolite signals that had been quantum-mechanically simulated. Metabolite concentrations were estimated using the QUEST method (jMRUI software (15,16)), which fits a time-domain model function, a combination of metabolite basis set signals, directly to the low signal-to-noise ratio (SNR) *in vivo* data (11). The metabolite basis set constitutes both the prior knowledge included in the model function and the starting values of the optimization procedure. The basis set signals can be given arbitrary lineshapes.

**Measured metabolite basis set.** To set up the measured metabolite basis set, 11 metabolite solutions were prepared (19–22). Asp, Cr, Cho, GABA, Glc, Glu, Gln, NAA, Tau, Lac, and Ins were dissolved separately in 10 mL phosphate-buffered aqueous solutions, pH = 7.0 ± 0.1, at a final concentration of 100 mM, except for Asp, Cr, and Glu solutions, which were 50 mM. The metabolites were purchased from Sigma-Aldrich (Saint Quentin Fallavier, France). Trimethylsilylpropanesulfonic acid sodium salt (DSS) and sodium formate were added as chemical-shift references. For better and longer storage, sodium azide was added as a preservative (18). The metabolite signals were acquired at 7 T (horizontal Biospec system; Bruker BioSpin MRI, Ettlingen, Germany) using The Point Resolved Spectroscopy Sequence (PRESS). It is essential that the measured basis set be obtained using acquisition parameters identical with those used in the *in vivo* study (see under ‘*In vivo* study’) at the physiological pH and temperature. To minimize  $T_1$  relaxation effects, the fully relaxed *in vitro* metabolite signals were acquired by using a long repetition time ( $TR = 10$  s). The 11 signals were Lorentzian line broadened, resulting in spectra with resonance linewidths of 10 Hz, to ensure that the linewidths *in vitro* matched those *in vivo*. The residual water and internal reference resonances were removed using HLSVD (Hankel-Lanczos singular value decomposition algorithm) (23). Twenty-five spectral components were used to model the filtered-out resonances. The spectra of the measured metabolite basis set are displayed in Fig. 1.

**Simulated basis set.** For the simulated metabolite basis set, all 11 signals were quantum-mechanically simulated at 7 T for the *in vivo* experimental protocol (PRESS sequence,  $TE$  of 20 ms, bandwidth of 4 kHz, 4096 data points, Lorentzian lineshape, damping factors of 30 Hz) with NMR-SCOPE (24). The current version of NMR-scope accommodates only  $T_2$  effects during the acquisition time of the MR sequence.

The spin Hamiltonian parameters (number of spins, chemical shifts,  $J$ -couplings) were obtained from Ref. (25) and refined when necessary. The spectra of the simulated metabolite basis set are displayed in Fig. 1.

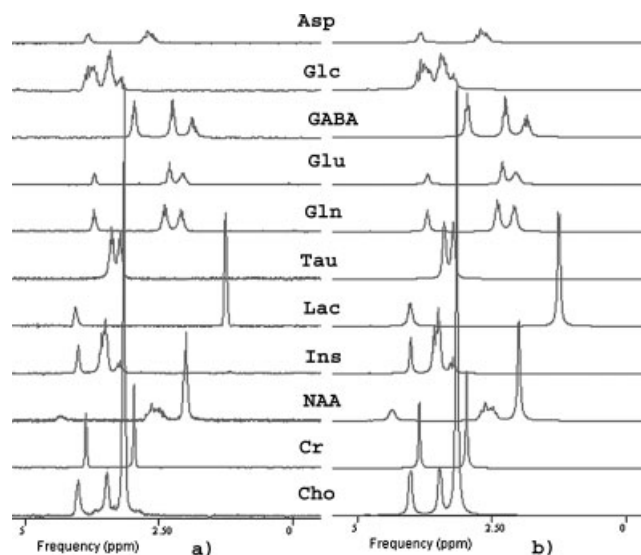


**Figure 1.** Spectra of the metabolite basis sets: (a) measured at 7 T using a PRESS sequence with  $TE = 20$  ms,  $TR = 10$  s; (b) quantum-mechanically simulated with NMR-scope using the same sequence.

## Direct comparisons of metabolite basis sets

Figure 1 shows the spectra of the measured and simulated basis sets used in this study. The differences in intensity, frequency, and damping factor between the measured and simulated spectra are a natural consequence of the difference between the ways of creation. To investigate possible deviations between the two basis sets, each signal (spectrum) of the simulated basis set was compared with its measured counterpart. This comparison was achieved by fitting the simulated basis set signal of each metabolite to its measured counterpart, using QUEST, and by inspecting the residue for any visible evidence of serious mismatch. The free parameters in the latter fit were: the damping factors, the frequencies, and the amplitudes. The ‘fit-adapted’ signal corresponding to the  $m^{\text{th}}$  metabolite  $x_m^{\text{adapt}}(t)$  is described by the following expression:

$$x_m^{\text{adapt}}(t) = x_m(t) \Delta a_m \exp(\Delta \alpha_m t) \exp(j2\pi \Delta f_m t) \quad (1)$$

where  $x_m(t)$  is the raw signal corresponding to the  $m^{\text{th}}$  metabolite,  $\Delta a_m$ ,  $\Delta \alpha_m$  and  $\Delta f_m$  represent, respectively, the adjustments in terms of amplitude, damping factor, and frequency when fitting a simulated basis set signal to its measured counterpart, and  $j^2 = -1$ . In the present version of QUEST, the damping adjustments of the signals are Lorentzian and were restricted to 5 Hz.

## Monte Carlo simulations

The influence of the metabolite basis sets on the quantification results was addressed with the aid of

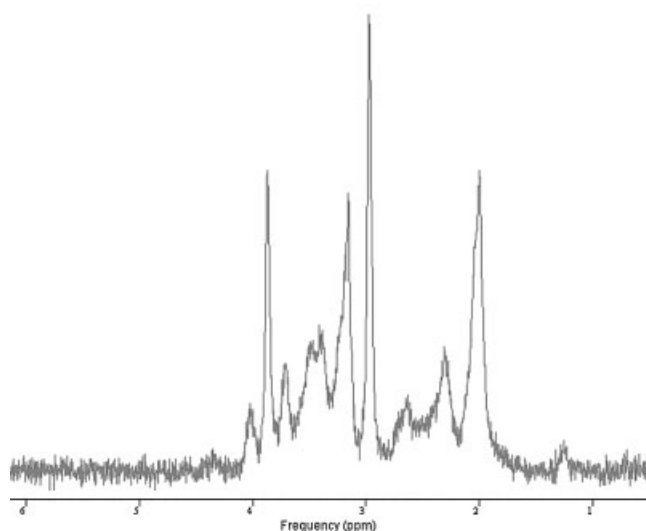


**Figure 2.** Example of the Fourier transform of a signal (weighted sum of the 11 measured metabolite signals acquired at 7 T, SNR 24:1,  $\Delta a = 10$  Hz) used in the first Monte Carlo study.

Monte Carlo simulations. A signal mimicking an *in vivo* rat brain signal acquired at 7 T was created for the **first** Monte Carlo study. It consisted of a weighted sum of the 11 measured metabolite signals (Fig. 2). Each summed signal was weighted according to the *in vivo* intensity ratios NAA:Cr:Cho:Ins:Glu:Gln:GABA:Glc:Asp:Lac:Tau = 8.5:7.5:1.9:3.5:6.5:3.5:2:1.6:1.9:0.6:5.8. These metabolite intensity ratios (concentrations) correspond to the published values for normal adult rat brain (19,26–27). The resulting signal was Lorentzian line broadened to mimic an *in vivo* signal acquired at 7 T in the rat brain. Two different linewidths ( $lw = \alpha/\pi$ , where  $lw$  is the linewidth and  $\alpha$  is the damping factor) were chosen. Each extra damping value of 5 Hz and 10 Hz led to total damping factors of 35 Hz and 40 Hz, respectively. These values differ slightly from the damping factors ( $\alpha = 30$  Hz) used to set up the two metabolite basis sets. A total of 270 realizations of white Gaussian-distributed noise were added to both signals. Two noise levels were chosen corresponding to SNRs of 60:1 and 24:1 compared with the Cr amplitude. The SNR of 24:1 corresponds approximately to the SNRs measured *in vivo*.

A **second** Monte Carlo study was performed differing from the first in that the simulated MRS signal was made up of the components of the simulated basis set. The metabolite intensity ratios, the linewidths, the number of noise realizations, and the noise levels were the same as those used in the first Monte Carlo study.

For each set of 270 signals of each Monte Carlo study, quantification was carried out with QUEST using both basis sets. When a quantification method based on a non-linear least-squares algorithm is used, it is well known that the starting values given to the fitting algorithm can influence the estimates because of the risk of convergence to local minima. To reduce this influence,

we used the fit-adapted version of the basis sets in the quantifications of the Monte Carlo signals. Consequently, in the **first** Monte Carlo study, QUEST was combined with the fit-adapted version of the simulated basis set and the raw measured basis set. Conversely, in the **second** Monte Carlo study, the raw simulated basis set and the fit-adapted version of the measured basis set were used. The free parameters in the fits were: the damping factors, the frequencies, and the amplitudes. The zero-order phase and the dead time were fixed to zero in the quantification algorithm.

Cramér–Rao lower bounds (CRLB) were computed using the true parameters (28,29). An estimate was considered relevant when the corresponding CRLB was found to be below 15% of the estimate. The mean of the relevant estimates and the error values corresponding to four standard deviations ( $\pm 2$  SD, 95% confidence interval) were computed.

To eliminate the difficulties related to the background accommodation, no background signal was added to the signals used for the Monte Carlo studies. The purpose of this study was to compare the influence of the two basis set approaches on the metabolite concentration estimates and not the influence of the background accommodation strategy.

### **In vivo study**

Experiments were performed on a 7 T horizontal Biospec system (Bruker BioSpin MRI) equipped with a gradient set (12 cm diameter, 400 mT/m maximum amplitude). A birdcage coil (72 mm inner diameter) and a surface coil (15 mm diameter) were used for excitation and reception, respectively.

Healthy adult rats (Sprague–Dawley, 200–250 g in weight, eight animals) were anesthetized by inhalation of isoflurane (Abbott Laboratories, Rungis, France; 2.5% concentration in a mixture of 50% oxygen and 50% nitrous oxide). Body temperature was maintained at 37°C with circulating warm water. A pressure probe was used to monitor the respiratory cycle. Experiments were conducted by procedures approved by the institutional animal care and ethical committee of the university.

Acquisitions were performed using a short-*TE* PRESS sequence ( $TE = 20$  ms,  $TR = 5$  s, bandwidth of 4 kHz, 4096 data points, 128 averages, acquisition time of 11 min, 15 signals) combined with outer volume suppression. The water signal was suppressed by variable power radio-frequency pulses with optimized relaxation delays (VAPOR) (30). All first- and second-order shim terms were adjusted using FASTMAP (Fast, Automatic Shimming Technique by Mapping Along Projections) (31) for each volume of interest (VOI) positioned in the centre of the left part of the rat brain (Fig. 3). Shimming resulted in unsuppressed water spectral linewidths of 7–12 Hz. Eddy current compensation and static magnetic

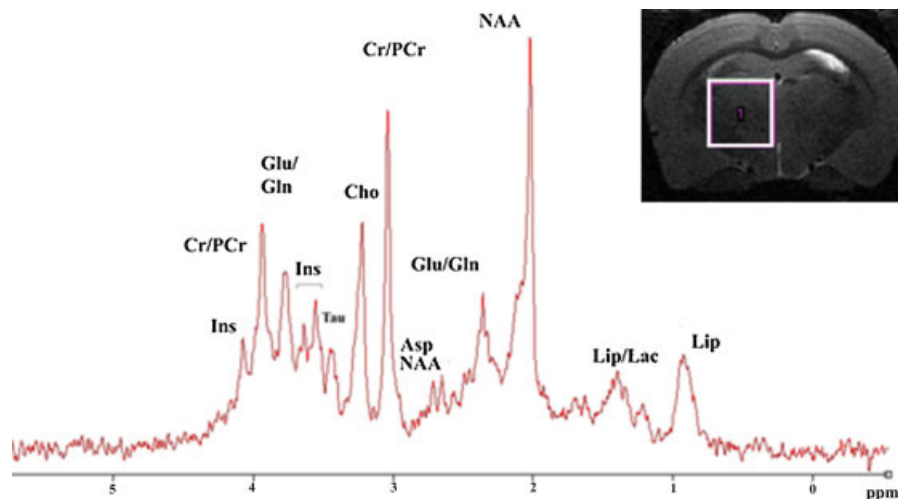


**Figure 3.**  $T_2$ -weighted RARE image of a rat brain obtained at 7 T, with the VOI positioned in the center of the brain and the *in vivo*  $^1\text{H}$  NMR spectrum acquired from the corresponding region using a PRESS sequence ( $TE = 20$  ms,  $TR = 5$  s).

field drift correction, based on navigator techniques provided with the PRESS sequence by Bruker, were applied during the acquisitions.

The localization of the VOIs was based on  $T_2$ -weighted RARE (Rapid Acquisition with Relaxation Enhancement) images ( $TR/TE = 6200/61$  ms, field of view =  $25 \times 19$  mm<sup>2</sup>, slice thickness 0.5 mm, echo spacing 19.2 ms, RARE factor = 8, matrix =  $256 \times 192$ ) (Fig. 3). The VOI size (3.5 mm<sup>3</sup>) was adjusted to fit the anatomical structure of the selected brain region and to minimize partial volume effects.

Residual water components were removed from the *in vivo* signals using HLSVD (25 spectral components were used for modeling).

The *in vivo* metabolite concentrations were estimated using the two raw basis sets. The free parameters in the fits were: the damping factors, the frequencies, and the amplitudes. The zero-order phase and the dead time were fixed to zero in the quantification algorithm. Because a surface coil was used, the *in vivo* metabolite concentration estimates were set proportional to the total creatine (Cr + PCr) concentration, used as an internal reference, which was assumed to be 7.5 mmol/kg wet weight (19,26–27).

Background accommodation was performed using ‘Subtract’-QUEST (11). The background estimates depend on the number of truncated data points and the prior knowledge provided by the metabolite basis set. In the present version of ‘Subtract’-QUEST, this number is chosen by the user using an empirical approach, so that the phased real-part of the background spectrum estimates is positive and the main resonances of the macromolecule are well identified. If a number that is too small is chosen, the background estimates will be underestimated; conversely a number that is too large leads to overestimation of the background estimates. In this study, the optimum number of truncated data points was defined

for each *in vivo* signal and found to be in the range 20–25 (corresponding to a duration of  $\sim 5.6$  ms).

The accuracy of the estimates was assessed using CRLB (11). An estimate was regarded as relevant when the corresponding CRLB was below 15% of the estimate. The mean of the relevant estimates and the corresponding error values ( $\pm 1$  SD, 70% confidence interval) were computed. The averaged relative differences between the concentration estimates using the two basis sets, over the 15 signals, were also computed.

The estimates of metabolite concentration obtained using the two metabolite basis sets were compared statistically using a paired two-tailed Student’s *t* test. In the statistical analysis,  $P < 0.05$  was considered significant, and  $P < 0.01$  and  $P < 0.001$  were considered highly significant. The 95% confidence intervals for the true mean differences were also evaluated.

## RESULTS

### Direct comparisons of metabolite basis set

For each fit, the root mean square error of the residue incurred when fitting the simulated basis set signal to its measured counterpart was computed and normalized to the amplitude of the corresponding measured signal (Table 1). These subsequent fittings led to adjustment of the amplitudes, frequencies, and damping factors of the simulated signals of each metabolite to their measured counterparts (Table 1). The adjustments of the frequencies were smaller than 4 Hz, confirming good agreement between the signals of the basis sets in terms of *J*-coupling and the chemical-shift values. The adjustments of the damping factors of the simulated basis set signals were Lorentzian and less than 5 Hz, corresponding to enlargement of the linewidths of the peaks of  $\sim 1.6$  Hz.

**Table 1.** Root mean square errors of the residues incurred when fitting the simulated basis set signals to their measured counterparts normalized to the amplitude of the corresponding measured signals [frequency adjustments ( $\Delta f$ ) and damping factor adjustments ( $\Delta\alpha$ ) are also displayed]

	Gln	Ins	Glc	Cho	Glu	Tau	GABA	NAA	Asp	Lac	Cr
Normalized root mean square error (%)	1.2	1.4	1.8	2.2	1.2	2.4	3.3	2.6	3.9	4.8	2.3
$\Delta f$ (Hz)	-1.2	2.7	3.6	-2.1	-1.0	-0.1	1.1	-0.4	0.4	-3.4	-0.1
$\Delta\alpha$ (Hz)	2.8	1.0	4.5	4.8	0.0	5.0	0.0	5.0	4.9	0.0	0.0

The adjustments of the amplitudes represent the differences between the amplitudes of the measured and simulated basis set signals. The amplitudes of the simulated signals are given by the number of protons in the metabolites. The amplitudes of the measured signals strongly depend on the acquisition parameters (type of coil, voxel size, number of acquisitions, the receiver gain of the coil,  $TR$ ,  $TE$ , concentration of each metabolite in the solution, magnetic field strength, etc). As the amplitude adjustments are related so closely to the acquisition protocol, we considered that these values did not have any relevance and are not displayed in Table 1.

No serious mismatch in the residues was observed. The relative differences, which are key indicators of the minimum differences to be expected between the

metabolite concentration estimates obtained using the two basis sets, were below 5%.

## Quantification results

**Monte Carlo studies.** The relative influences of the two metabolite basis sets were evaluated by comparing the respective standard deviations and the bias of the amplitude estimates. In the **first** Monte Carlo study (based on the signal containing a weighted sum of 11 measured signals), all the metabolites were clearly identified using either of the two metabolite basis sets, even with small SNRs and large damping factors (Fig. 4). For each

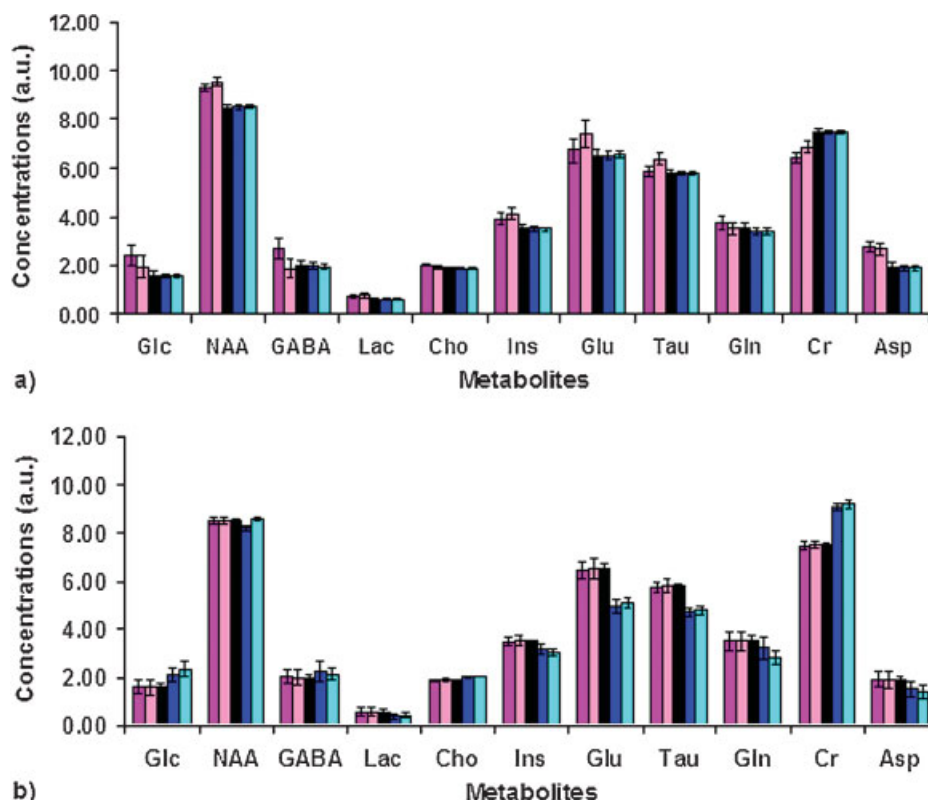


**Figure 4.** Means of the relevant concentration estimates (a.u.) and the corresponding error bars ( $\pm 2SD$ ) for a SNR of 24:1. Quantifications were performed with QUEST combined with the measured [dark ( $\Delta\alpha = 10$  Hz) and light ( $\Delta\alpha = 5$  Hz) blue bars] or the simulated [dark ( $\Delta\alpha = 10$  Hz) and light ( $\Delta\alpha = 5$  Hz) pink bars] metabolite basis set for: (a) the first Monte Carlo study (the signal consisting of a weighted sum of 11 measured signals) and (b) the second Monte Carlo study (the signal consisting of a weighted sum of 11 simulated signals). The black bars represent the true metabolite concentrations and the corresponding CRLBs ( $\pm 2$  CRLBs;  $\Delta\alpha = 10$  Hz).

metabolite, the bias (difference between the mean value of the concentration estimates and the true concentration) was expressed as a percentage of the true concentration. A positive bias corresponds to an 'overestimation' of the concentration estimate compared with the true value, and a negative bias to an 'underestimation' of the concentration estimate. In this study, a large overestimation of the estimated amplitudes of the metabolites with low concentrations was obtained when the simulated basis set was used: Asp (~40%), Lac (~30%), Glc (~40%) and GABA (~30%). Also, a slight overestimation of NAA (~8%), Ins (~11%), Glu (~13%), Tau (~8%) and Gln (~7%) was observed when the simulated basis set was used. When the standard deviations were expressed as a percentage of the mean values of the concentration estimates, they were found to be between 0.5% and 5% for most of the metabolites: NAA, Cho, Cr, Tau, Ins, Glu, Gln, GABA, Asp, and Lac. As expected, larger standard deviations (for example, 18% for Glc, 10% for Lac, 9% for Asp) were observed with the lower SNRs and larger linewidths. The standard deviations were in good agreement with the CRLBs (correctly calculated from the true parameters).

Conversely, in the second Monte Carlo study (based on the signal containing a weighted sum of 11 simulated signals), biased estimates were obtained when the measured metabolite basis set was used: Glc (~30%), Lac (~30%), Asp (~20%), Cr (~20%), Glu (~20%), Tau

(~18%), GABA (~6%), Ins (~9%), and Gln (~8%) (Fig. 4). The standard deviations of the concentration estimates were not significantly different for the two approaches. They were between 0.5% and 5% for most of the metabolites. The standard deviations were in good agreement with the CRLBs (correctly calculated from the true parameters).

**In vivo study.** The high quality of the multislice  $T_2$ -weighted images of the rat brain provided accurate and reproducible positioning of the VOI. In Fig. 3, the displayed  $^1\text{H}$  NMR spectrum shows the spectral quality consistently achieved in our study. In addition to the commonly observed metabolites (NAA, Cr and Cho), Ins, Tau, Gln, Glu, Asp, Glc, and GABA were discernible in the central region of the rat brain. Using a reasonable scan time was used, the SNR turned out to be sufficient for reliable quantification with QUEST.

QUEST quantification results, obtained for an *in vivo* rat brain signal using the measured and simulated basis sets, are shown in Fig. 5. Good smooth approximations of the background signals were estimated. The main resonances of the background signal (dashed line) were well identified: both lipid resonances (0.9 and 1.3 ppm) and the three principal resonances of macromolecules (around 2.0–2.5 ppm, 3.0–3.2 ppm, and 3.5–3.9 ppm). The subtract-QUEST method involves the metabolite basis set in the estimation of the background. Because

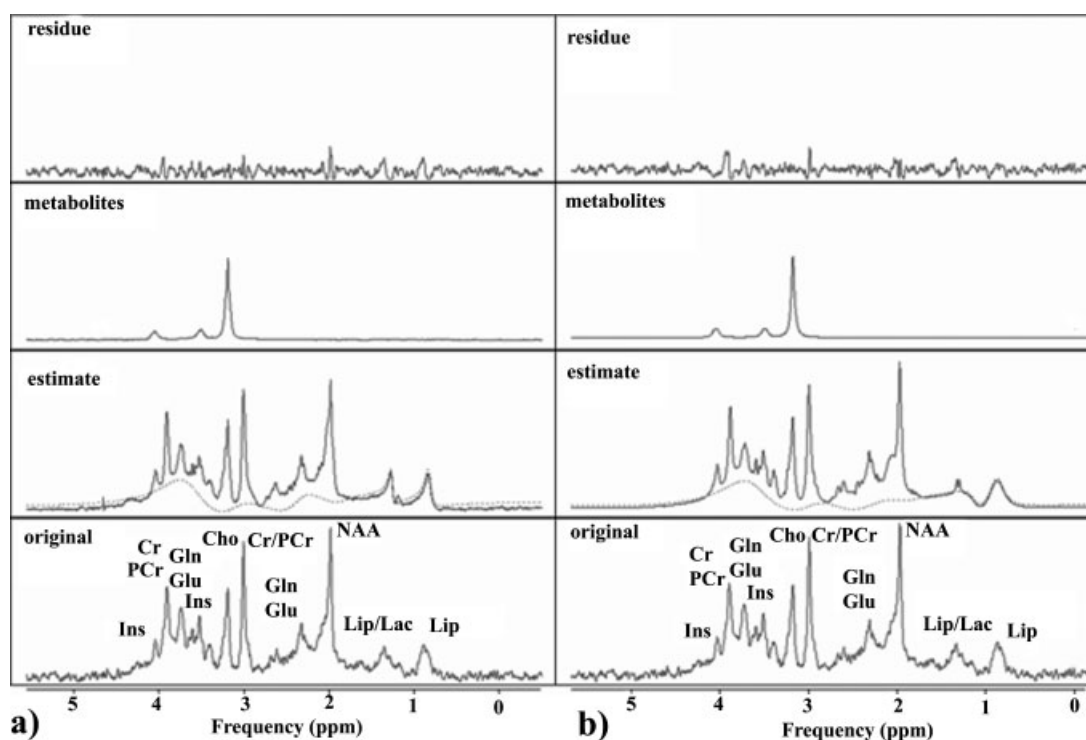


**Figure 5.** Results of QUEST quantification using: (a) the measured metabolite basis set; (b) the simulated basis set. From bottom to top: original spectrum acquired *in vivo* at 7 T in the centre of the rat brain (PRESS,  $TE = 20$  ms,  $TR = 5$  s); estimated spectrum and background (dashed line); Cho estimated spectrum; and residue.

the basis set used in each approach was slightly different (see under 'Comparisons of metabolite basis sets' in Discussions and Conclusions), the resulting background estimates were slightly different too, as can be seen in Fig. 5.

An estimate was considered relevant when the corresponding CRLB was below 15% of that estimate. Applying this criterion, 10 of the 11 metabolite concentration estimates were relevant for both approaches. Quantification of barely-present metabolites, such as Lac, was not relevant because of its low *in vivo* concentration and strong correlation with the lipid resonances at 1.3 ppm.

The mean values (in mmol/kg wet weight) and the corresponding standard deviations ( $\pm 1$  SD) of the metabolite concentration estimates using the raw basis sets are shown in Table 2. The standard deviations revealed the inter-individual metabolite differences and were in the same range for the estimates using the two metabolite basis sets. The averaged relative differences are independent of the inter-individual metabolite differences, but reveal the differences between the concentration estimates obtained using the two basis sets. These values were  $\sim 20\%$  for all the metabolites (Table 2). When a paired two-tailed Student's *t* test was used, significant differences between the mean concentration estimates obtained using the two approaches were observed for Cho ( $P < 0.001$ ) and NAA, Glu ( $P < 0.01$ ). By referring to the 95% confidence interval for the mean differences, the true mean differences are likely to lie between 0.59 and 3.19 for NAA, 0.33 and 0.58 for Cho, and 0.26 and 0.88 for Glu. Consequently, the normalized bounds with respect to the corresponding mean of the metabolite concentration obtained using the measured basis set were 5.7% to 30.8% for NAA, 15.5% to 31.0% for Cho, and 3.9% to 28.1% for Glu.

## DISCUSSIONS AND CONCLUSIONS

The influence of measured and quantum-mechanically simulated metabolite basis sets on metabolite concentration estimates was compared using Monte Carlo simulations and an *in vivo* study.

### Direct comparisons of metabolite basis sets

Each signal (spectrum) of the simulated basis set was compared with its measured counterpart. No serious differences were observed between our measured and simulated basis set signals, and the signals of our two basis sets were similar in terms of *J*-coupling and chemical-shift properties. The normalized root mean square differences were below 5% and accounted for the differences in the way each basis set signal was obtained. The latter expressed the differences between the experimental acquisitions and the quantum-mechanical simulations: for instance, the pulse shapes, the relaxation time effects, the lineshapes, and the magnetic field inhomogeneities. Furthermore, these differences accounted for the noise in the measured basis set as well as errors related to removal of water and internal reference. The adjustments in terms of frequencies and damping factors did not alter the lineshapes of the simulated basis set signals because their lineshapes were already Lorentzian and the values of these adjustments were small (Table 1).

### Monte Carlo studies

Although the direct comparison of the two basis set signals revealed only small differences, in the Monte Carlo simulations, several metabolite concentration estimates showed biases, especially Asp, Lac, Glc, and

**Table 2.** Mean values and corresponding standard deviations of the relevant metabolite concentration estimates obtained from 15 signals of rat brains using the two raw metabolite basis sets<sup>a</sup>

Metabolite	This study (n = 15 signals)			Literature	
	Measured basis set	Simulated basis set	% (averaged relative differences)	Biochemical rat assays	<i>In vivo</i> rat brain
NAA	10.31 $\pm$ 1.48	8.38 $\pm$ 0.84	18%	4.7–9.7	8.3 $\pm$ 0.5; 7.6–10.0; 5.7–8.1
Cho	1.91 $\pm$ 0.18	1.46 $\pm$ 0.18	23%	—	0.7 $\pm$ 0.1; 1.2–1.7
tCr (Cr+PCr)	7.50	7.50	—	8.5–9.7	7.7; 8.3–9; 6.0
Ins	3.93 $\pm$ 0.40	3.85 $\pm$ 0.55	16%	—	4.1 $\pm$ 0.5; 1.8–3.2
Tau	5.87 $\pm$ 1.01	5.25 $\pm$ 0.94	18%	5.0–7.4; 1.6–6.6	4.2 $\pm$ 0.6; 8.1–10.8
Glu	6.65 $\pm$ 0.92	7.76 $\pm$ 0.76	21%	7.4–12.5	8.6 $\pm$ 0.7; 8.7–11.2; 6.5–8.7
Gln	3.47 $\pm$ 0.59	3.59 $\pm$ 0.74	20%	2.1–5.6; 3.8–4.7	1.2 $\pm$ 0.3; 2.8–3.5
Glc	1.56 $\pm$ 0.27	1.95 $\pm$ 0.62	30%	0.96	3.5 $\pm$ 0.4; 2.8–3.5
Asp	1.78 $\pm$ 0.55	2.22 $\pm$ 0.81	22%	1.5–2.7; 2.5–3.8	1.4 $\pm$ 0.4; 1.2–2.4
GABA	3.16 $\pm$ 0.47	3.79 $\pm$ 0.36	20%	0.8–2.3; 1.3–1.7	1.1 $\pm$ 0.3; 0.9–1.1

<sup>a</sup>The averaged relative difference, over the 15 signals, between the concentration estimates using both basis sets is also displayed. tCr (Cr + PCr) was used as internal reference [7.5 mmol/kg<sub>ww</sub> (kg wet weight)] and consequently has no error bar. For comparison, published metabolite concentrations from biochemical rat brain assays and *in vivo* rat brains are also displayed (26–27, 34).

GABA. A ready explanation is that these metabolites were among the most weakly represented in the signal. Furthermore, the spectral peaks of Asp, Glc, and GABA are widely spread and their resonances overlap considerably with those of more abundant metabolites, which make their quantification difficult.

The fitting of a model function to an experimental signal leads to biased estimates when the model function is not appropriate. Thus, by building the signal from the measured metabolite signals (**first** Monte Carlo study), quantification with the simulated basis set is unavoidably biased, and quantification with the measured basis set yields estimates consistent with the true values (and vice versa) (Fig. 4). As we have already mentioned, when using a quantification method based on a non-linear least-squares algorithm, it is well known that the starting values provided can influence the estimates because of the risk of convergence to local minima. The metabolite basis sets constitute both the prior knowledge included in the model function and the starting values of the optimization procedure. To better disentangle the effect on the estimates of the starting values given to the fitting algorithm from those related to the basis set itself, we provided the quantification algorithm with the fit-adapted basis set signals. As the fit adaptation did not fundamentally alter the signal lineshapes, the use of the fit-adapted version of the simulated (measured) basis set in the quantifications of the **first** (**second**) Monte Carlo study had no effect on the subsequent fits other than providing slightly different starting values. Quantifications using the raw basis sets in place of the fit-adapted ones were also performed (data not shown). The relative differences between the mean values of the concentration estimates obtained using the raw basis sets and the corresponding fit-adapted basis sets were 1–10%. Note that, for the quantifications with the raw basis sets, an internal reference was needed to scale the concentration estimates. Consequently, total Cr (Cr + PCr) was used and its concentration was set to 7.5 mmol/kg wet weight. Consequently, fit adaptation of the basis sets was only a way of better evaluating the effect of the basis set itself on the estimates by disentangling the effects of the starting values given to the fitting algorithm. Of course, when a simulated basis set is set up, the measured basis set is presumably not available.

In our study, no correction of lineshapes of the basis set signals (for example, by applying the QUALITY method (32)) was performed before the quantification process because the relative differences, reported in Table 1, were deemed to be small. However, the present version of QUEST adjusts the damping of the basis set signals in a Lorentzian manner.

As no background signal was included in the Monte Carlo simulation signals and the influence of the starting values given to the fitting algorithm was reduced by using the fit-adapted basis set signals, the explanation of the biases may be related to the differences reported in Table 1 spectral overlap and SNR and differences in

lineshapes (33). The biases incurred are also a natural consequence of the mismatch between the metabolite basis set signals and the Monte Carlo signals, especially the differences in lineshape and the differences related to water removal. In conclusion, the results were optimal when the basis set used for the fit was the same as that used to simulate the Monte Carlo signals.

### *In vivo* study

In the analysis of *in vivo* data, the lineshapes of both basis sets are flawed. Moreover, the true metabolite concentrations are unknown, and, accordingly, comparison of the results obtained with these basis sets is difficult.

Regardless of the above shortcomings, 10 metabolites were well identified using the two basis sets. Quantification of Lac was deemed not relevant due to its low *in vivo* concentration and strong correlation with the lipid resonances at 1.3 ppm. No statistically significant differences between the concentration estimates using the two approaches were observed, except for NAA, Cho, and Glu. However, as the low end of the confidence intervals of the true mean differences between the estimates obtained using both basis sets for NAA and Glu were too small to be considered significant, we conclude that the difference in results obtained with the two basis sets was probably not large enough to be scientifically relevant. For Cho measured *in vivo*, the study showed a large significant difference in the quantification results obtained by the two basis sets, which may be scientifically relevant. There are several possibilities to account for this difference. As is well known, *in vivo* metabolite quantification of short-*TE* signals is hampered by an unknown broad overlapping background spectrum. In this case, quantification becomes difficult. Moreover, as already mentioned, when a quantification method based on a non-linear least-squares algorithm is used, the starting values can influence the estimates because of the risk of convergence to local minima. In addition, the prior knowledge included in the model function has a direct effect on the estimates. The raw basis set signals used as starting values and prior knowledge for the *in vivo* quantifications present differences that are the natural consequence of their ways of creation. As previously mentioned, the latter expressed the differences between the experimental acquisitions and the quantum-mechanical simulations: for instance, the pulse shapes, the relaxation time effects, the lineshapes, and the magnetic field inhomogeneities. Furthermore, these differences accounted for the noise in the measured basis set as well as errors related to removal of water and internal reference.

As a consequence of the slightly different starting values and prior knowledge provided to the processing algorithm, the resulting background estimates differed slightly, leading to further differences between the metabolite concentration estimates. The averaged relative



differences were  $\sim 20\%$ . However, note that our concentration estimates with confidence intervals were consistent with values from the literature (Table 2). The latter were estimated from biochemical rat brain assays (26–27) and from quantification of *in vivo* rat brain spectra using LC-Model (26–27) and AMARES (34).

Quantifications using the fit-adapted basis sets in place of the raw ones were also performed for the *in vivo* study. When the fit-adapted basis sets were used, the averaged relative differences between the estimates obtained using the two approaches (simulated versus measured basis set) showed no improvement compared with those obtained with the raw basis sets. Consequently, the corresponding estimates were not reported in the paper. Moreover, as already mentioned, when a simulated basis set is being set up, the measured basis set is presumably not available.

Methods are being developed to automate the procedure for disentangling the background signal from the metabolite signal (35–37). To reduce the effects of the basis sets on the estimates, future investigations will make the disentanglement procedure more independent of the prior knowledge introduced by the metabolite basis sets, starting with a lineshape adaptation of the measured/simulated basis set signals to the *in vivo* signals. The effect of removing the residual water signal in the measured basis set and the *in vivo* signals needs to be considered too.

The two basis sets used in our study present the following advantages (+) and drawbacks (–).

Measured basis set:

- + A subset of the *in vivo* experimental conditions is automatically taken into account.
- + The metabolite concentration estimates are automatically and partially compensated for in the spin–spin relaxation effects occurring during the MR sequence duration. The *in vivo* signal weighted by  $\exp(-TE/T_{2vivo})$  was modeled by a weighted sum of measured metabolite signals themselves weighted by  $\exp(-TE/T_{2vitro})$ .  $T_{2vivo}$  and  $T_{2vitro}$  correspond to the *in vivo* and *in vitro* transverse relaxation times, respectively, of the metabolite considered.
- A new basis set has to be acquired for any new experimental protocol. Preparing the solutions and acquiring the basis set signals is tedious and time-consuming.
- The basis set signals have some noise.

Simulated basis set:

- + The basis set can easily and quickly be simulated for any experimental protocol using NMR-SCOPE or similar computer programs.
- Some experimental conditions were not taken into account. For instance, the current version of NMR-scope accommodates only spin–spin relaxation effects during the acquisition.

As our *in vivo* concentration estimates, with confidence intervals obtained using both basis sets, were in good

agreement with values in the literature, and as the *in vivo* study showed that, in general, the differences between the estimates obtained with the two basis sets were not statistically significant or scientifically important, a simulated basis set can be used in place of a measured basis set.

## Acknowledgements

The experiments were performed on the ANIMAGE platform, Lyon, France. We are grateful to Dr H. Ratiney and Dr M. Cabanas for fruitful discussions.

## REFERENCES

1. Salvan AM, Ceccaldi M, Confort-Gouny S, Milandre C, Cozzone PJ, Vion-Dury J. Correlations between cognitive status and cerebral inositol in Alzheimer-type dementia. *J. Neurol.* 1998; **245**(10): 686–688.
2. Clarke CE, Lowry M. Systematic review of proton magnetic resonance spectroscopy of the striatum in parkinsonian syndromes. *Eur. J. Neurol.* 2001; **8**(6): 573–577.
3. Butteriss DJ, Ismail A, Ellison DW, Birchall D. Use of serial proton magnetic resonance spectroscopy to differentiate low grade glioma from tumefactive plaque in a patient with multiple sclerosis. *Br. J. Radiol.* 2003; **76**(909): 662–665.
4. Ranjeva JP, Confort-Gouny S, Le Fur Y, Cozzone PJ. Magnetic resonance spectroscopy of brain in epilepsy. *Childs Nerv. Syst.* 2000; **16**(4): 235–241.
5. Simister RJ, McLean MA, Barker GJ, Duncan JS. A Proton Magnetic Resonance Spectroscopy Study of Metabolites in the Occipital Lobes in Epilepsy. *Epilepsia* 2003; **44**(4): 550–558.
6. Zubler F, Seeck M, Landis T, Henry F, Lazeyras F. Contralateral medial temporal lobe damage in right but not left temporal lobe epilepsy: a  $^1\text{H}$  magnetic resonance spectroscopy study. *J. Neurol. Neurosurg. Psychiatry* 2003; **74**(9): 1240–1244.
7. Flugel D, McLean MA, Simister RJ, Duncan JS. Magnetisation transfer ratio of choline is reduced following epileptic seizures. *NMR Biomed.* 2006; **19**(2): 217–222.
8. Cudalbu C, Cavassila S, Montavont A, Ryvlin P, Briguet A, Graveron-Demilly D. Study of pilocarpine model of epileptic rats at 7T by magnetic resonance spectroscopy. In *Proceedings of the International Society of Magnetic Resonance in Medicine, 14<sup>th</sup> Scientific Meeting and Exhibition*, Seattle, Washington, 2006; 2530.
9. Lyoo IK, Renshaw PF. Magnetic resonance spectroscopy: current and future applications in psychiatric research. *Biol. Psychiatry* 2002; **51**(3): 195–207.
10. Leclerc X, Huisman TA, Sorensen AG. The potential of proton magnetic resonance spectroscopy ( $^1\text{H}$ -MRS) in the diagnosis and management of patients with brain tumors. *Curr. Opin. Oncol.* 2002; **14**(3): 292–298.
11. Ratiney H, Sdika M, Coenradie Y, Cavassila S, van Ormondt D, Graveron-Demilly D. Time-domain semi-parametric estimation based on a metabolite basis-set. *NMR Biomed.* 2005; **18**(1): 1–13.
12. Provencher SW. Estimation of metabolite concentrations from localized *in vivo* proton NMR spectra. *Magn. Reson. Med.* 1993; **30**(6): 672–679.
13. Soher BJ, Young K, Govindaraju V, Maudsley AA. Automated spectral analysis III: application to *in vivo* proton MR spectroscopy and spectroscopic imaging. *Magn. Reson. Med.* 1998; **40**(6): 822–831.
14. Slotboom J, Boesch C, Kreis R. Versatile frequency domain fitting using time domain models and prior knowledge. *Magn. Reson. Med.* 1998; **39**(6): 899–911.
15. <http://www.mrui.uab.es/mrui/>
16. Naressi A, Couturier C, Devos JM, Janssen M, Mangeat C, de Beer R, Graveron-Demilly D. Java-based graphical user interface for the MRUI quantitation. *MAGMA* 2001; **12**(2–3): 141–152.

17. Young K, Govindaraju V, Soher BJ, Maudsley AA. Automated spectral analysis. I. Formation of a prior information by spectral simulation. *Magn. Reson. Med.* 1998; **40**(6): 812–815.
18. <http://s-provencher.com/pages/lcmodel.shtml>
19. Cudalbu C, Cavassila S, Ratiney H, Beuf O, Briguet A, Graveron-Demilly D. Localized proton MRS at 7 T in the rat brain: estimated metabolite concentrations and T<sub>2</sub> relaxation times. In *Proceedings of the European Society of Magnetic Resonance in Medicine and Biology, 22<sup>th</sup> Annual Scientific Meeting and Exhibition*, Basel, 2005; 207.
20. Cudalbu C, Cavassila S, Ratiney H, Grenier D, Briguet A, Graveron-Demilly D. Estimation of metabolite concentrations of healthy mouse brain by Magnetic Resonance Spectroscopy at 7 Tesla. *C.R. Chimie* 2006; **9**: 534–538.
21. Cudalbu C, Cavassila S, Ratiney H, Beuf O, Briguet A, Graveron-Demilly D. Metabolite concentrations of healthy mouse brain by magnetic resonance spectroscopy at 7 Tesla. In *Proceedings of IEEE Engineering in Medicine and Biology Society, IEEE EMB*, Shanghai, 2005; 1392–1395.
22. Cudalbu C, Cavassila S, Ratiney H, Beuf O, van Ormondt D, Graveron-Demilly D. Metabolite concentration estimates in the rat brain by magnetic resonance spectroscopy using QUEST and two approaches to invoke prior knowledge. In *ProRISC, IEEE Benelux*, Veldhoven, 2005; 609–614.
23. Pijnappel WWF, van den Boogaart A, de Beer R, van Ormondt D. SVD-based quantification of magnetic resonance signals. *J. Magn. Reson.* 1992; **97**: 122–134.
24. Graveron-Demilly D, Diop A, Briguet A, Fenet B. Product operator algebra for strongly coupled spin systems. *J. Magn. Reson.* 1993; **A101**: 233–239.
25. Govindaraju V, Young K, Maudsley AA. Proton NMR chemical shifts and coupling constants for brain metabolites. *NMR Biomed.* 2000; **13**(3): 129–153.
26. Pfeuffer J, Tkac I, Provencher S, Gruetter R. Toward an *in vivo* neurochemical profile: quantification of 18 metabolites in short-echo-time (1)H NMR spectra of the rat brain. *J. Magn. Reson.* 1999; **141**(1): 104–120.
27. Tkac I, Rao R, Georgieff MK, Gruetter R. Developmental and regional changes in the neurochemical profile of the rat brain determined by *in vivo* <sup>1</sup>H NMR spectroscopy. *Magn. Reson. Med.* 2003; **50**(1): 24–32.
28. Cavassila S, Deval S, Huegen C, van Ormondt D, Graveron-Demilly D. Cramer-Rao bounds: an evaluation tool for quantitation. *NMR Biomed.* 2001; **14**(4): 278–283.
29. Cavassila S, Deval S, Huegen C, van Ormondt D, Graveron-Demilly D. The beneficial influence of prior knowledge on the quantitation of *in vivo* magnetic resonance spectroscopy signals. *Invest Radiol.* 1999; **34**(3): 242–246.
30. Tkac I, Starcuk Z, Choi IY, Gruetter R. In vivo <sup>1</sup>H NMR spectroscopy of rat brain at 1ms echo time. *Magn. Reson. Med.* 1999; **41**(4): 649–656.
31. Gruetter R. Automatic localized *in vivo* adjustment of all first- and second-order shim coils. *Magn. Reson. Med.* 1993; **29**(6): 804–811.
32. de Graaf AA, van Dijk JE, Bovée WM. QUALITY: quantification improvement by converting lineshapes to the Lorentzian type. *Magn. Reson. Med.* 1990; **13**(3): 343–357.
33. Marshall I, Bruce SD, Higinbotham J, MacLulich A, Wardlaw JM, Ferguson KJ, Seckl J. Choice of spectroscopic lineshape model affects metabolite peak areas and area ratios. *Magn. Reson. Med.* 2000; **44**(4): 646–649.
34. Mierisova S, van den Boogaart A, Tkac I, Van Hecke P, Vanhamme L, Liptaj T. New approach for quantitation of short echo time *in vivo* <sup>1</sup>H MR spectra of brain using AMARES. *NMR Biomed.* 1998; **11**: 32–39.
35. Cudalbu C, Cavassila S, Rabeson H, van Ormondt D, Graveron-Demilly D. Localized proton magnetic resonance spectroscopy at 7 Tesla in the rat brain: metabolite concentration estimates using QUEST and two approaches to accommodate the background. In *ProRISC, IEEE, Benelux*, Veldhoven, 2006; 136–140.
36. Rabeson H, Ratiney H, Cudalbu C, Cavassila S, Capobianco E, de Beer R, van Ormondt D, Graveron-Demilly D. Signal disentanglement in *in vivo* MR spectroscopy: by semi-parametric processing or by measurement? In *ProRISC, IEEE, Benelux*, Veldhoven, 2006; 176–183.
37. Cudalbu C, Bucur A, Graveron-Demilly D, Beuf O, Cavassila S. Comparison of two strategies of background-accommodation: influence on the metabolite concentration estimation from *in vivo* magnetic resonance spectroscopy data. In *Proceedings of IEEE Engineering in Medicine and Biology Society, IEEE EMB*, Lyon, 2007; 2077–2080.